SURVIVABILITY • SUSTAINABILITY • MOBILITY
SCIENCE AND TECHNOLOGY
SOLDIER SYSTEM INTEGRATION

TECHNICAL REPORT
NATICK/TR-98/016

AD_____

GLINT FIELD TRIAL RESULTS AND APPLICATION TO GLINT THRESHOLD DISTANCE ALGORITHM

by

William J. Chevalier

and

Brian Kimball

March 1998

Final Report

October 1996 - September 1997

U.S. ARMY SOLDIER SYSTEMS COMMAND
NATICK RESEARCH, DEVELOPMENT AND ENGINEERING CENTER
NATICK, MASSACHUSETTS 01760-5000

SCIENCE AND TECHNOLOGY DIRECTORATE

DISCLAIMERS

The findings contained in this report are not to be construed as an official Department of the Army position unless so designated by other authorized documents.

Citation of trade names in this report does not constitute an official endorsement or approval of the use of such items.

DESTRUCTION NOTICE

For Classified Documents:

Follow the procedures in DoD 5200.22-M, Industrial Security Manual, Section II-19 or DoD 5200.1-R, Information Security Program Regulation, Chapter IX.

For Unclassified/Limited Distribution Documents:

Destroy by any method that prevents disclosure of contents or reconstruction of the document.

REPORT DOCUMENTATION PAGE

Form Approved
OMB No. 0704-0188

1. AGENCY USE ONLY *(Leave blank)*	2. REPORT DATE	3. REPORT TYPE AND DATES COVERED
	March 1998	Final October 1996 - September 1997

4. TITLE AND SUBTITLE
GLINT FIELD TRIAL RESULTS AND APPLICATION TO GLINT THRESHOLD DISTANCE ALGORITHM

5. FUNDING NUMBERS
AH 98

6. AUTHOR(S)
William J. Chevalier and Brian Kimball

7. PERFORMING ORGANIZATION NAME(S) AND ADDRESS(ES)
U.S. Army Soldier Systems Command
Natick Research, Development & Engineering Center
Kansas Street, ATTN: SSCNC-YA (W. Chevalier)
Natick, MA 01760

8. PERFORMING ORGANIZATION REPORT NUMBER
NATICK/TR-98/016

9. SPONSORING/MONITORING AGENCY NAME(S) AND ADDRESS(ES)

10. SPONSORING/MONITORING AGENCY REPORT NUMBER

11. SUPPLEMENTARY NOTES

12a. DISTRIBUTION/AVAILABILITY STATEMENT
Approved for public release, distribution unlimited

12b. DISTRIBUTION CODE

13. ABSTRACT *(Maximum 200 words)*

This report describes the results and applications of the U.S. and U.K. joint venture glint field trials conducted in the summer, 1997, in Malvern, England, under Army operations information exchange agreement IEA-A-A-96-1998. As a model validation and verification effort, the Field Trial results obtained would be used to improve the integrity of an existing U.S. glint threshold algorithm. Software adjustments would tentatively be made to the existing algorithm to improve glint threshold distance calculation accuracy, making the modified model a better iterative eye armor design tool.

The combined effects of atmospheric extinction and turbulent distortion C_N^2 play a major role in degrading the optical image or electo optical energy transmitted along its sun-to-reflector-to-observer optical path. A range of relative reflectivity coefficients corresponding to reflecting surface solar incidence angles describe the optical reflectivity characteristics of the surface in question. Incorporating these effects and the detector (eye) power/angular resolution concepts, spectrally resolved and integrated contrast ratios of reflecting source to background, which are independent of solar fluctuations, can generate more accurate visual threshold domains and a more useful reflecting surface design tool.

14. SUBJECT TERMS				15. NUMBER OF PAGES
GLINT	REFLECTIVE TECHNOLOGIES	SURVIVABILITY	THRESHOLD	47
MODEL	OPTICAL PATH	OPTICAL REFLECTANCE	FIELD TRIALS	16. PRICE CODE
DISTANCE	EYE ARMOR	REFLECTION COEFFICIENTS	ALGORITHMS	

17. SECURITY CLASSIFICATION OF REPORT	18. SECURITY CLASSIFICATION OF THIS PAGE	19. SECURITY CLASSIFICATION OF ABSTRACT	20. LIMITATION OF ABSTRACT
Unclassified	Unclassified	Unclassified	

Table of Contents

Table of Contents (Cont'd)

Table of Contents (Cont'd)

List of Figures

List of Tables

Preface

This report describes the results and applications of the U.S. and U.K. joint venture glint field trials conducted the summer of 1997 in Malvern, England, under the Army Operations Research Information Exchange Agreement IEA-A-A-96-1448. As a model validation and verification effort, the field trial results are to be used to improve the integrity of an existing U.S. glint threshold algorithm. Software adjustments would tentatively be made to the existing algorithm to improve glint threshold distance calculation accuracy, making the modified model a better iterative eye armor design tool.

Spectrally resolved and integrated techniques were applied to values of solar glint to background intensity measured within the imaging detector's dynamic range to generate glint to background contrast ratios over a range of distances from reflecting source. An attempt was made to filter out atmospheric extinction values associated with different humidity band levels. Random noise effects to the glint and background propagating continuous wave-fronts (signature) due to ground level atmospheric turbulence defined as C_N^2, the refractive index structural function parameter, inevitably caused variability in the glint-to-background-intensity values measured. Every measure was taken to minimize experimental design background noise. Because of time limitations and the effects of a wet summer, the field trials results were adversely affected.

The authors would like to extend their appreciation to Mr. Dean-Michael Sutherland and Mr. Harry Kirejczyk, Operations Research Analysts, Science and Technology Directorate; and Ms. Landa Hoke, Research Physicist, Survivability Directorate, for their constructive editing of this report.

Special thanks is extended to Ms. Marcia Lightbody, our Chief Editor, for her very constructive editing comments in helping to finalize the report.

We are deeply indebted to our United Kingdom (U.K.) counterparts Dr. R.C. Hollins and Dr R.I. Young for allowing us to conjointly conduct the glint trial runs at their optics test facilities at the Defence Evaluation and Research Agency (DERA) Optics Test Facilities, Malvern, U.K. These gentlemen played a significant role in contributing to the level of success that was achieved, offering key and timely comments as needed.

GLINT FIELD TRIAL RESULTS AND APPLICATION TO GLINT THRESHOLD DISTANCE ALGORITHM

SUMMARY

This report describes the results and applications of the United States and United Kingdom glint field trials conducted the summer of 1997 in Malvern, England, under the Army Operations Research Information Exchange Agreement IEA-A-A-96-1448. As a model validation and verification effort, the field trial results obtained, when data are sufficient, are to contribute to improve the integrity of an existing U.S. glint threshold algorithm. Software adjustments are to tentatively be made to improve glint threshold distance accuracy making the modified model a better iterative design tool.

Spectrally resolved and integrative techniques were used to generate glint-to-background contrast ratios derived from solar intensity measurements taken by a charged coupled device (CCD) fixed-gain imaging detector at various distances from the reflecting eye armor sources during humidity-varying sunny days. The eye armor reflecting sources used for the field trials were the U.S. Army M-40 outsert dielectric stack cylindrical system and the United Kingdom (U.K.) tri-stimulus laser protective spherical system. Along with the use of neutral density filters, a 670 nm narrow band pass was used in conjunction with the cylindrical reflecting surface while an eye visual range filter (0.4-0.7 um) was used with the spherical reflecting surface to accommodate the detector's dynamic range.

Because the number of glint field trials conducted was limited due to time and weather constraints, the resulting data derived from the trials could not be nested within humidity bands. Thus the atmospheric extinction parameters could not be evaluated. For the unaided eye the extent of the visibility of solar glint is derived for each reflecting surface.

Using the cylindrical eye armor reflecting surface, it was found that glint is quite visible at 1100 meters with a contrast ratio of 10. The projected visual threshold using a 1.1 contrast ratio is in the 2000 to 2500 meter range based on U.K. estimates. A statistical curve fitting projection through the derived data wasn't feasible because of the large variability in the residuals caused by atmospheric turbulence (C_N^2) over the relatively large observer-to-reflecting-source distance considered.

Regarding the use of the spherical eye armor reflecting surface, the contrast ratio is approximately 1.2 at 100 meters. Glint disappears beyond the distance of 200 meters from the reflecting source at the 1.1 contrast ratio. These values were based on the application of a statistical curve fit model to the data.

Because of the inability to evaluate the total atmospheric extinction parameter associated with different humidity levels, complicated by the atmospheric turbulence effects on the propagating glint signatures, the data obtained from the glint field trials are insufficient in scope to warrant verifying and validating the existing glint threshold algorithm. However, the ability to discern glint at a range of 2000-to-2500 meters or more warrants further investigation in assessing the potential of glint hazard.

GLINT FIELD TRIAL RESULTS AND APPLICATION TO GLINT THRESHOLD DISTANCE ALGORITHM

1. INTRODUCTION

A need exists to investigate the optical glint phenomena by determining the degree to which the reflective, optical surfaces of eye armor systems raise the level of detection during sunny days and moonlit nights. Thus, the ultimate question to be answered is,"do specular reflecting surfaces increase the range at which visual detection occurs"? If the answer proves positive, under what combat scenarios and appropriate solar environmental conditions does glint present a significant survivability hazard to the dismounted soldier operating in open, wooded, and desert terrain.

The reflected eye visible solar spectral (0.4 - 0.7μm) to background intensity ratios were measured by placing a Charged Coupled Device (CCD) imaging detector at various distances from the eye wear along a sun-reflector-observer optical path during humidity varying sunny days. The glint-to-background contrast ratios are independent of variations in solar brightness since the glint and background solar reflections change proportionally. The field measurement model used by the U.K. assumes glint as a point source and the background as an extended object.

This report describes the results and applications of the U.S. and U.K. joint venture glint field trials conducted the summer of 1997 in Malvern, England, under Army Operations Research Information Exchange Agreement IEA-A-A-96-1448. As a model validation and verification effort, the field trial results obtained would be used to improve the integrity of an existing U.S. glint threshold algorithm. Software adjustments would tentatively be made to the existing algorithm to improve glint threshold distance calculation accuracy, making the modified model a better iterative eye armor design tool.

1.1 ANALYTICAL STRUCTURE

The analysis discussed in this report will be considered for improving the capability of the existing U.S. glint threshold distance model to assist in the evaluation of the application of reflective technologies to eye armor. By adjusting the existing glint threshold calculation algorithm to improve glint threshold distance calculation accuracy, the designer can better modify the eye armor surface optics and more closely correlate changes in threshold distance due to changes to the surface reflection coefficients.

The eye armor program will function in concert with other soldier system component programs in the development of an evolving soldier system that will satisfy mission and threat requirements. For example, according to Lieutenant Colonel Wilfred 'Bud' Irish, U.S. Army Program Manager for Small Arms, the U.S. Army is conducting several new optical initiatives designed to enhance soldier lethality. One of these initiatives is developing a new family of Anti-Reflection Devices to counteract glint enhancement due to laser hardening of optical surfaces including those of eye armor.

1.2 TECHNICAL OBJECTIVE

1. To conduct a set of glint field trials for verifying and validating an existing glint threshold calculation model.
2. To determine the degree to which reflective optical surfaces of eye armor protective systems increase the level of glint, given the factor influences of surface reflection geometry and atmospheric extinction effects due to different levels of humidity.

1.3 TECHNICAL APPROACH

Glint-intensity versus distance data were acquired for both the U.S. Army M-40 outsert dielectric stack cylindrical system and the U.K. tri-stimulus laser protective spherical system. The laser protective systems were located at various measured distances from the data acquisition system. At each distance, images were recorded of the glinting surface and background using a charge coupled device (CCD) camera and associated frame-grabber software.

Quantitative glint data are obtained by using image processing software to perform line scans at locations of interest within the image. A line scan gives *relative* intensity in terms of grey levels for the pixels of interest. These can range in value from 0 to 255. A line scan can be performed anywhere within an image. In this way, contrast values can be obtained for glint and more than one type of background within a single image. Verification of the U.K. model requires relative intensity values for the glint and background in order to calculate contrast values.

A lux-meter was used to measure ground level solar source intensity at the time of recording of each image. These measurements were taken in close proximity to the glinting surface.

This study dealt with glint detection by eye only. Therefore, the human eye photopic response region of 0.4 - 0.7 μm was the only region of the electromagnetic spectrum for which experimental data were obtained.

1.3.1 TRIAL RUNS

The experimental set-up is shown in Figure 1. The glinting surface was secured to a tripod and oriented such that the solar or sky glint was directed through the window of an enclosure (not shown) in which the data acquisition system was located. Images were recorded using a fixed-gain CCD camera and associated software. A lux-meter was used to record source intensity. The dynamic range of the instrument was extended by placing neutral density (ND) filters between the camera optics and the scene to be recorded.

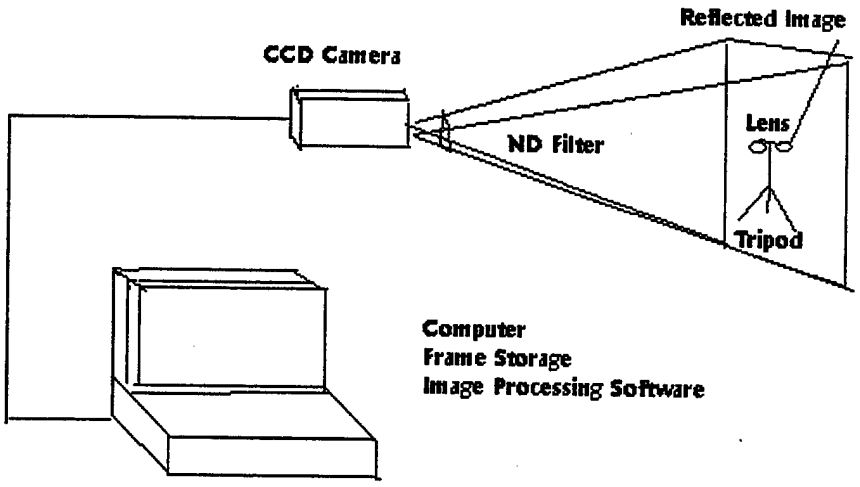

Figure 1. Experimental Setup Used to Record Glint Data

1.3.2 Experimental Procedure

During the performance of the trial-runs a number of issues arose that represented potential sources of experimental uncertainty. These included:

-Operation within the dynamic range of the data acquisition system,
-Measurement-system versus eye spectral response,
-Source variations and atmospheric considerations,
-Angle of incidence.

These issues were dealt with as they arose and are briefly described below.

1.3.2.1 Operation Within the Dynamic Range of the Data Acquisition System

In most instances eye armor specular reflection was too great to be recorded with a CCD camera against a natural background, such as bushes, grass or sand. This is because the CCD camera was saturated when the incident glint was not attenuated. Saturation occurs when the camera takes in light that is too intense for the CCD chip to measure. Thus the incident light is outside the dynamic range of the CCD camera. No pertinent information can be extracted from a saturated image. The glint intensity was brought within the dynamic range of the camera by darkening the image field with ND filters. However, the background became too dark to measure. A self-adjusting camera was not useful, because the frame-to-frame variation in camera compensation rendered image comparison impossible. This problem was addressed by using a fixed-gain camera and recording two images, one of which was attenuated to a known degree. Relative glint intensity was extracted from the attenuated image and compensated by the known degree to which the ND filter darkened the image. Background intensity was obtained from the nonattenuated image.

This technique is based on the assumption that the time interval between the recording of the two images was short enough that the scene did not change. In practice it was possible to record two images within about 30 seconds. For relatively stable conditions this period was acceptable.

1.3.2.2 Measurement System Versus Eye Spectral Response

The photopic (daytime) spectral response of the eye differs from that of the silicon CCD camera. The peak sensitivity of the eye is centered at about 550 nm while that of silicon is centered at about 950 nm. Thus, the camera will record glint reflections associated with wavelengths that the eye cannot see. These wavelengths may be of interest in the case of vision enhancement devices, but this study was limited to glint detection by eye only.

This issue was resolved by use of band-pass filters. Images were recorded using a narrow band-pass filter at 667 nm and also a photopic multi-wavelength filter. A wavelength of 667 nm is strongly reflected by both the U.S. dielectric stack M-40 outsert and the U.K. tri-stimulus lens. This wavelength is also visible to the eye. A photopic filter changes the spectral response of the CCD camera to that of the eye.

The use of the single-line filter is more desirable than the photopic filter from a variable control perspective because the glinting surfaces have their own spectral characteristics. That is, during the course of the experiment, as the declination angle of the sun increases, proportionally more shorter-wavelength light is attenuated by the atmosphere. The lenses reflect longer wavelengths more efficiently, thus more incident light is reflected to contribute to the glint. With a multi-wavelength photopic filter, the changing spectral source characteristics add another unwanted variable to the study. The photopic filter is more appropriate, however, from a realistic perspective, and more apt to provide the desired information (note in results that effects of the photopic filter on accuracy are unclear).

1.3.2.3 Source Variation and Atmospheric Considerations

In addition to the changes in source spectral characteristics discussed in the previous section, there was the issue of source intensity fluctuations. These can be due to changes in cloud cover, humidity, azimuth angle, temperature and wind-sheer. However, the comparative glint-source-to-background spectrally resolved intensity measurements taken were independent of source intensity variations since source and background intensities change in proportion. Measurements taken using the eye filter would be more sensitive to spectral shifts due to source variations caused by changes in atmospheric conditions.

Since atmospheric extinction effects on transmitted solar spectral signatures directly correspond to changes in the level of aerosols, dust particles, water vapor and temperature, a need existed to monitor continuously the micro-meterological conditions during the progress of the trial runs. A weather station monitored atmospheric conditions throughout the course of the experiments.

Temperature and wind sheer can combine to create a scintillation effect caused by what are commonly referred to as "heat-waves". These are essentially localized changes in the refractive index of air. This causes the glint intensity to fluctuate when observed at a distance. The experimental uncertainty introduced by this effect requires a minimum threshold number of images be take at each measurement distance in order to make the distribution of values most representative across the gaussian spectral noise distribution.

1.3.2.4 Angle of Incidence

Lens surface reflectivity is a function of angle of incidence. Whereas the location of the sun moves through the course of the data acquisition process, this movement was a matter of concern. A rather simple technique was devised to record angle of incidence, which utilized a line-of-sight, a plumb bob and a protractor. For these experiments, however, this source of uncertainty was expected to be relatively small. In an effort to reduce time between image recordings, no corrections were attempted for variations in angle of incidence. This issue is mentioned here for purposes of completeness.

1.4 BACKGROUND RATIONALE

The degree to which glint is a military hazard to the dismounted soldier wearing ballistic laser eye armor protection is not presently clear. There is some evidence, however, that a need exists to continue to investigate antireflection and low reflection technologies to reduce the effects of the hazard. The benefit to the soldier of a glint reduction scheme would be to allow soldiers to perform their missions with lower probability of revealing their presence to the enemy.

A contract was awarded to Raytheon to develop a computer code that calculates glint threshold distance from a reflecting source. It was based on the application of point source theory to reflecting sources, i.e., eye armor reflections at a distance from reflecting source to observer, which invokes the application of the inverse square law. It was assumed that the background reflection intensity remains constant over the distance since the number of background point source reflections increases proportionally with the square of the distance from the background reflecting source. The model also assumed worst case scenario, i.e., desert conditions where humidity levels are low, and thus atmospheric extinction effects on reflected glint signature are negligible. The optical path considered was sun-reflecting surface-observer.

The level of reflected spectral energy from a reflecting source would vary with the product of the weighted average zenith solar spectral intensity value, zenith angle coefficient and the reflecting surface coefficients. The resulting glint threshold locus of points calculated by the model algorithm was based on this product, the background brightness level, the inverse square law, and a glint threshold of 100 times the minimum discernible threshold seen by the naked eye. Theoretically, the lowest discernible glint threshold to the observer is when the reflecting source to background brightness contrast ratio equals 1.02, based on scientific studies.

This model can be used as an iterative design tool for measuring the effects of design modifications to the optical surface properties of eye armor. Changes in calculated glint threshold distances would correspond to changes in the optical surface properties of eye armor, since surface reflectivity coefficients would be modified over a given range of solar incidence angles.

The purpose for running the glint threshold trials was to verify the accuracy of the existing glint threshold distance algorithm. The field trials would provide data that reflect the factor influences of atmospheric extinction due to humidity and surface geometry on the intensity of reflected light from the eye wear. By adjusting the existing glint threshold algorithm to reflect these changes, glint threshold distance calculation accuracy would be more realistic.

1.5 HISTORICAL PERSPECTIVE

According to Beth Redden, US Army Research Laboratory, Fort Benning, Georgia, recent literature about soldier survivability does not seem to include glint as a survivability issue. There is no mention of glint in the Infantry Lessons Learned Database at Fort Benning. The soldier survivability parameter assessment list does not include glint under "Component II: Reduce Detectability" which assesses a system's physical signature as it affects the system's detection level by threat forces. Other signatures, such as the system's silhouette, thermal signature, olfactory signature, and acoustical signature are covered. How many times has glint from soldiers' optical devices or other reflecting equipment revealed their positions and led to engagements by an adversary on his terms? Based on available research and information from subject matter experts, no one seems to have an answer to that question, even from force-on-force training exercises.

However, a brief examination of historical battlefield accounts does provide some insights into the glint issue. Four compelling combat accounts of target detection due to glint reflections are provided to illustrate the significance of reducing glint to enhance soldier survivability.

1. Glint had a major impact on the results of the battle of Gettysburg. Reflections from the Confederate's equipment alerted the Union's General Warren to their position below him on "Little Round Top". The reinforcements he sent for were just able to turn the tide in that pivotal battle. The ability to remain undetected is paramount to survival or completion of the mission. Today, no military force would think of going into the field without camouflaging their troops and equipment.

2. Moshe Dayan, the Israeli general, got his famous eye patch when a sniper saw reflections of the sun from his binoculars. Modern optical systems produce the highest quality images, give protection from an enemy's offensive lasers and allow you to see into the thermal range. Unfortunately, these same optics also have the ability to betray their own position by reflecting light. Glint is an obvious signature that can key even a marginally trained counter observer to detect troops and equipment. Reflections from optical systems or vehicle lighting can compromise operational security. Operational security means we, not the enemy, determine the time and place of engagement.

3. At the battle of Stalingrad during World War II, Russia's top sniper, Vasili Zaitsev, credited with more than 200 kills, won a famous three day duel with the German top sniper, Major Zossen, by looking for and targeting the reflection from the German's rifle scope. If they can't see you they can't shoot you.

4. During the 1942 battle of Guadalcanal, the Japanese army's second attack on Henderson Airfield was planned as a surprise assault from the dense jungle to the south of the field. The U.S. forces were warned about the impending attack after a member of the 7th Marine patrol noticed a glint reflection emanating from a hilltop. The source of the reflection was a pair of binoculars held by a Japanese officer. The U.S. forces were shifted in time to repel the "surprise" attack.

2. RESULTS

Because the number of glint field trials conducted was limited due to bad weather and time constraints, humidity bands could not be defined from the limited database from which to derive extinction coefficients. Also, atmospheric turbulence was present and significantly affected the results of the conducted field trials. The multi-wavelength photopic filter used during the trial runs may have introduced some unwanted variation due to spectral shifts over the course of taking data. For the unaided eye, the limits on the visibility of solar glint are derived from the data obtained using each reflecting surface.

2.1 CYLINDRICAL SURFACE (Dielectric Stack)

Glint is quite visible at 1100 meters where the contrast ratio equals approximately 10.0 (see Figure 1). Glint thresholds with a 1.1 contrast ratio within the 2.0-2.5 km range from the reflecting source. The viewing angle is 3 through 45 degrees.

2.2 SPHERICAL GOGGLES (Ables)

The contrast ratio is approximately 1.2 at the 100 meter distance (see Figure 2). Glint disappears beyond the distance of 200 meters from the reflecting source at a 1.1 threshold contrast ratio. The viewing angle was 90 degrees in the horizontal direction.

3. ANALYSIS OF RESULTS

The reflecting source to background contrast ratio measurements were taken over a range of distances from the Natick cylindrical dielectric stack and U.K. spherical (Ables) reflecting surfaces using a CCD image detection system. The measurements were taken over several days at the 1.2 kilometer laser optics range in Malvern, U.K., during the early 1997 summer months as weather conditions permitted. Virtually all the data was taken from 1100 to 1800 hours each day the glint trials were executed. The level of humidity was not considered as a controlling factor because the execution of the trial runs was primarily influenced by a wet summer season in the U.K. Therefore, atmospheric extinction coefficients could not be derived from the data taken, which was one of our objectives.

The large variability in the cylindrical lens data, Table B-1, taken at the respective distances from the cylindrical reflector by the detector was primarily due to the low level atmospheric turbulence effects that became more pronounced over the distance the glint signal traveled. Each day that measurements were taken offered slightly different environmental conditions, which affected the level of scintillation in terms of distortion and tilt of the glint spectral energy wave front relative to the background reflection energy. Since the detector takes an instantaneous picture reading of the glint and background signature intensities, each ridden by a gaussian shaped spectral noise frequency, a minimum threshold number of readings needed to be taken at each measured distance to normalize the data spread in order to nullify the effects of scintillation or wave-front distortion. More data were needed to accomplish this end, but would have been irrelevant because of the extent of the variability of the data due to the atmospheric turbulence.

The cylindrical surface graph in Figure 2 depicts the relationship between contrast ratio and distance from cylindrical reflecting source and shows the effects of atmospheric turbulence. The average contrast ratio at 1100 meters is about 10. Because of the large random variation in the residuals, it was impossible to apply any curve-fitting techniques to predict a 1.1 contrast ratio

threshold distance with any degree of accuracy. However, if we apply equation A-14, identified in Appendix A: A.1.4.1.1, the threshold distance would be in the 2000 - 2500 meter range.

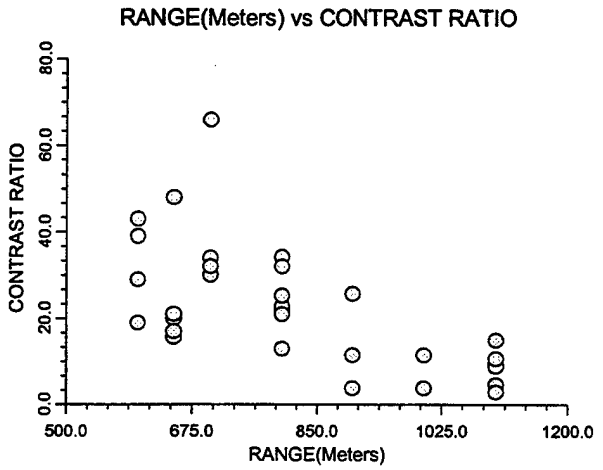

Figure 2: Cylindrical Surface

When taking measurements using the spherical reflecting source, the operators of the imaging detector used a photo-visual eye response filter. When examining the spherical lens data in Table B-2 in conjunction with Figure 3 below, we see little variability in the data taken at the respective distances from the spherical reflector because the data were taken over a 100 meter distance. Thus the atmospheric turbulence had little effect on the propagating glint signature.

The average contrast ratio at 100 meters was measured at 1.2. The projected visual threshold contrast value of 1.1 for the spherical reflecting surface calculates to be at about 200 meters, based on the application of the Bleasdale-Nelder statistical model [$Y=(A+BR)^{-1/C}$]. For example, using the spherical lens data in Table B-2 and applying the statistical model to generate a reasonable good curve fit, the resulting curve fit equation is estimated to be

$$Y = \text{Contrast Ratio (CR)} = (-.008989 + .00488\text{Range})^{-1/1.2768} \qquad (1)$$

Setting the Contrast Ratio to 1.1 which is close to the visual threshold value, the range calculates to be about 200 meters. See curve fit in Figure 4 below.

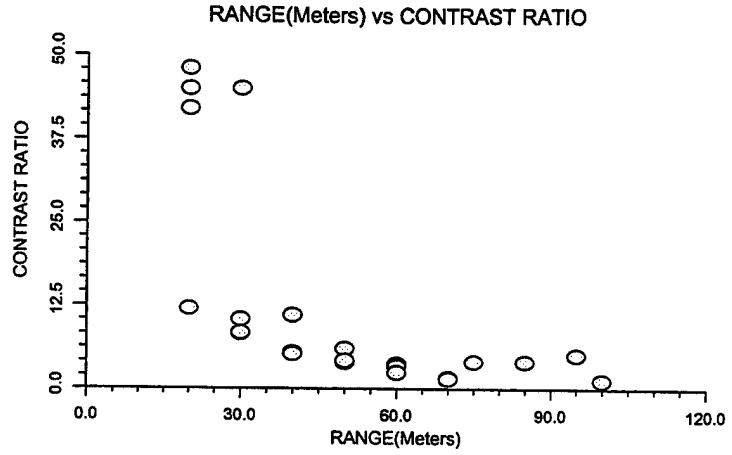

Figure 3: Spherical Surface

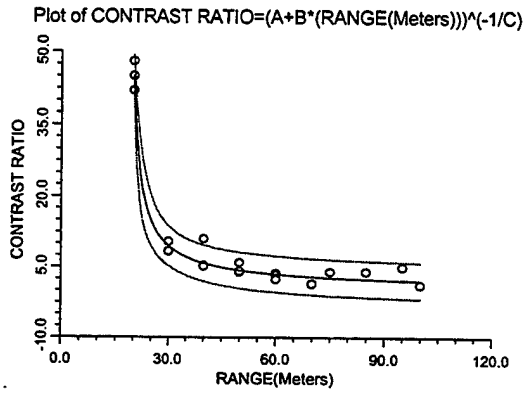

Figure 4. Cylindrical Surface: Contrast Ratio versus Range

The surface geometry and reflectivity optics differences of the spherical (Ables) and cylindrical (dielectric stack) surfaces indicate that the cylindrical surface contributes to a much larger glint threshold distance of about 2000 to 2500 meters from reflecting surface. This is based on projected calculations given that the measured contrast ratio is 10 at 1100 meters. As mentioned, the spherical surface contributes to a glint threshold distance calculation of 200 meters and a measured average contrast ratio of 1.2 at 100 meters. See photo-visuals in Appendix C.

Although the radii of curvature of both surfaces are similar in value, the optical surface properties of the dielectric stack cylindrical surface offer higher reflectivity coefficients over the range of reflection angles then do those of the spherical surface (Ables). The other contributing factor is the fact that the cylindrical surface has one radius of curvature compared to two for the spherical surface. This means that the spherical surface initiates a two dimensional divergence of the reflecting glint signature, which corresponds to reflected glint intensity correlating inversely to the square of the distance. In that context, the cylindrically reflected signature would have a single dimensional divergence because of the one radii, and would correlate inversely to the single power of distance. The rate of divergence in each case is inversely related to the square of the effective radius of curvature of the reflecting surface.

Other issues of concern that might have contributed somewhat to unwanted variability in the data include: a) background definition variations, b) control of glint incidence/reflection angle, c) measurement system versus eye spectral response, and d) operation within the dynamic range of the imaging detector.

It is very difficult to minimize or eliminate the random effects in taking the background imaging readings relative to the glint readings. Also, changes in the amount of glint reflected energy to change in incident angle become significant beyond an incidence/reflection angle of 45^0 to the reflecting surface, as evidenced by the relative luminosity versus reflection angle graph* depicted in Figure 5. These combined effects are probably more significant as distance between detector and reflecting source increases, i.e., cylindrical contrast ratio data (0-1100 meters) due to lack of control of experimental runs.

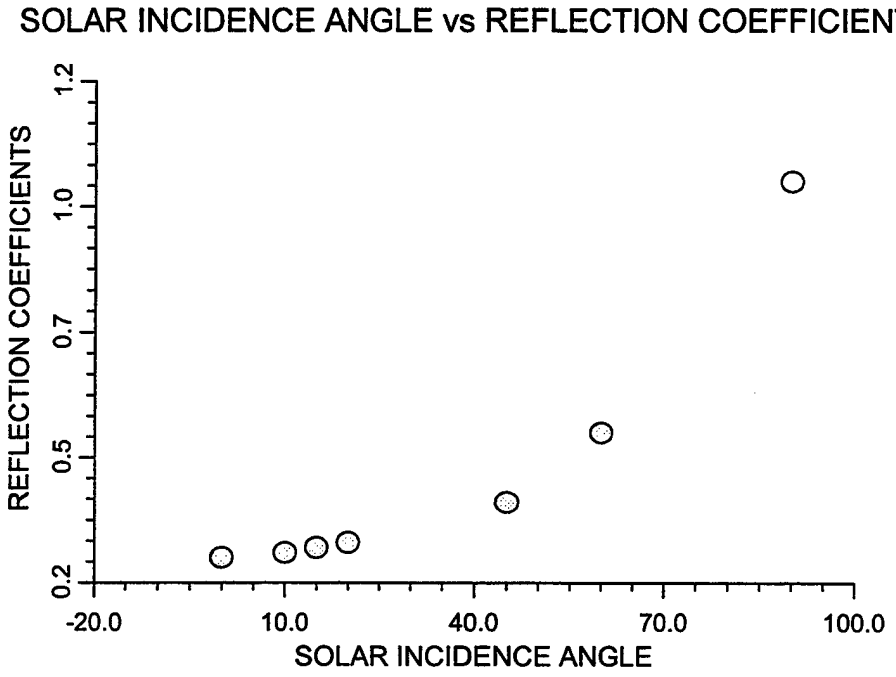

Figure 5: Normalized Reflectivity Coefficients of a Specular Reflecting Surface

It would have been ideal if an eye photo-spectral filter instead of the 670 nm filter was used while taking the cylindrical measurements, but readings were taken over a substantial distance and during the duration of the afternoons, which necessitated the use of the latter. Spectral shift occurs during the afternoon favoring the longer wavelengths, which are more efficiently reflected off the goggles.

It is absolutely necessary to operate within the dynamic range of the imaging detector to eliminate potential detector error in contrast ratio measurements. This factor alone could be a significant error contributor if some of the readings were saturated.

* Schmelz, Mark, "Reflections from the Sun-wind-Dust Goggles" Natick Labs, 07 May 1990, Natick, Ma.

4. CONCLUSIONS

(1) There were differences in the effects that the spherical and cylindrical reflecting surfaces and their associated optical reflectivity properties had on determining the glint visual threshold distance. Limits on the visibility of solar glint as viewed by the unaided eye were:

a) Spherical reflecting surfaces - Glint is visible with a 1.2 contrast ratio at 100 meters, but disappears just beyond 200 meters at a reflecting surface to background contrast ratio equal to 1.1.

b) Cylindrical reflecting surface - Glint is visible at 1200 meters at a contrast ratio of 10, but disappears within the 2000 to 2500 meter range.

(2) Atmospheric extinction effects on glint to background contrast ratios could not be derived. The repeated measurement glint contrast ratios generated from each reflecting surface over the respective distances considered were not nested within humidity bands due to time and weather constraints.

(3) Atmospheric turbulence created enough variation in the repeated contrast ratio measurements taken at the respective distances, particularly from the cylindrical reflecting surface, to substantially reduce any useful interpretation.

(4) Data obtained from the glint trials are insufficient in scope to warrant researchers being able to verify and validate the existing glint threshold calculation algorithm.

5. RECOMMENDATIONS

(1) Use the Raytheon Glint Threshold Distance Calculation Model as a "relative measures" iterative design tool in the application of appropriate reflective technologies to eye armor and other dismounted soldier reflective surfaces.

(2) Conduct a glint hazard assessment study (ongoing) to determine if there are any dismounted soldier scenarios where glint hazard is significant, and if so, what impacts would the effects of glint have on soldier survivability and ability to achieve the mission objective.

(3) If the glint hazard assessment study depicts circumstances where the effects of glint hazard are significant,

a) focus on the use of low- and antireflection technologies to negate effects of glint-producing soldier equipment worn by the dismounted soldier, and

b) conduct glint field trials to verify and validate existing or improved glint threshold models, and

c) conduct glint field trials to verify that there are combat situations where there is compromise to soldier mission objective and vulnerability due to significant differences in the glint detection times associated with recognizing scintillating and non-scintillating glint within the visual threshold distances from the reflecting surfaces.

Note: Improved mathematical model defined in Appendix A: section 1.4.1.3

6. LIST OF REFERENCES

1). RI Young, RC Hollins, T Holloway, "Simple Model for Predicting Glint to Background Contrast Ratios, Optical Glint Studies US and U.K. Joint Venture", DERA, U.K., July 1997.
2). Schmelz, Mark, "Reflections from the Sun-Wind-Dust Goggles" Natick Labs, 07 May 1990, Natick, MA.
3). Kreith, Frank, Principles of Solar Engineering. Washington, DC, McGraw Hill, 1978.
4). Forsythe, William Elmer, Smithsonian Physical Tables, 9th Revised Edition, Washington, D.C., Smithsonian Institution Press, 1956.
5). Erickson, Ronald, Visual Detection of Targets: Analysis and Review. U.S. Naval Ordnance Test Station, China Lake, CA., 1965 (AD612721).
6). Corson D.R., Lorrain P., "Introduction to Electromagnetic Fields and Waves", W.H. Freeman and Company, San Francisco and London, 1962.
7). Williams C.S., Bechlund O.A., "A Short Course for Engineers & Scientists" Wiley Inter-Science, New York, 1972.

APPENDIX A.

APPLICATION THEORY

1 APPLICATION THEORY

The following theory deals with the application of radiometric and photometric definitions of spectral energy transmitted along an optical path from sun to reflecting surface to observer. The interaction of solar spectral energy with a reflecting surface will be discussed in terms of radiometric phenomena such as: emissivity, reflectance, absorptance and transmittance, using the conservation of energy law. The effects of atmospheric extinction on transmitted solar spectral energy wavelengths within the eye response's visible region of 0.4 - 0.7μm, due to different levels of humidity, air born particles and atmospheric gases, will be mathematically defined. Since psychological stimuli and responses are involved in this experiment, it is fundamentally necessary to look at the photometric response of the eye to radiant flux density transmitted from a reflecting source to the observer, as the basis for interpreting the reflecting source to background solar glint contrast ratios. This discussion considers surface geometry effects on glint signature divergence and the contrast ratio measurements by an imaging detector.

1.1 RADIOMETRIC AND PHOTOMETRIC DEFINITIONS

When undertaking the study of radiometry and photometry, we assume the existence of an instrument called a radiometer. If radiant energy is incident upon a radiometric response surface of known area and orientation relative to its direction, then radiant energy is converted over to electrical energy in the radiometer as a stimulus response reaction. In the same context, the eye produces a bio-metric stimulus response reaction to radiant energy in the form of a photo electric conversion to sight.

Radiometric quantities are physical quantities that are expressed in energy and geometrical units. For purposes of this report the energy and geometric terms will be described in terms of rate of energy transmitted per unit area which is optically called radiant flux density. Thus the units can be expressed as watts/cm^2. The level of radiant flux density will be equated to the level of specular or glint reflection off of a mirror-like surface such as eye armor.

The retina of the eye of the human observer functions is a photoelectric receptor in response to radiant energy. Since perceptual response to physical stimuli is involved, the eye retinal receptor response to the visual wavelength spectrum of 0.38 - 0.74μm could be better defined as psycho-physical. We are dealing with a photo-metric response to a radiometric stimuli of solar spectral energy. In this context, light is a visual aspect of radiant energy of which the human observer is aware through the visual sensations which arise from the stimulation of the retina of the eye. Brightness is defined as that attribute of visual sensation by which an observer is aware of differences of observed radiant energy.

1.1.1 LUMINOUS ENERGY

When the human eye is used as an adapted photo-receptor response to a visual spectrum to measure the relative levels of brightness, a relative luminosity curve represented by the function $V(\lambda)$ is produced. A standard curve of this function has been established by international agreement and may be considered the relative spectral sensitivity of the average normal, light adapted human eye. Generally, to convert the visual spectrum of radiant energy to luminous energy Q, according to the spectral energy function U_λ we use the relative luminosity function $V(\lambda)$ as a weighting value in the following equations:

$$Q = K_M V(\lambda) U_\lambda \qquad \text{(A-1)}$$

or

$$Q = K_M \int_0^\infty V(\lambda) U_\lambda d\lambda \qquad \text{(A-2)}$$

where K_m is a constant that determines the size of the Q units. This equation provides the bridge to convert radiometric to photo-metric units.

The photopic spectral luminosity $V(\lambda)$ of the human eye as a function of wavelength of radiant energy* is depicted in Figure A1 as follows:

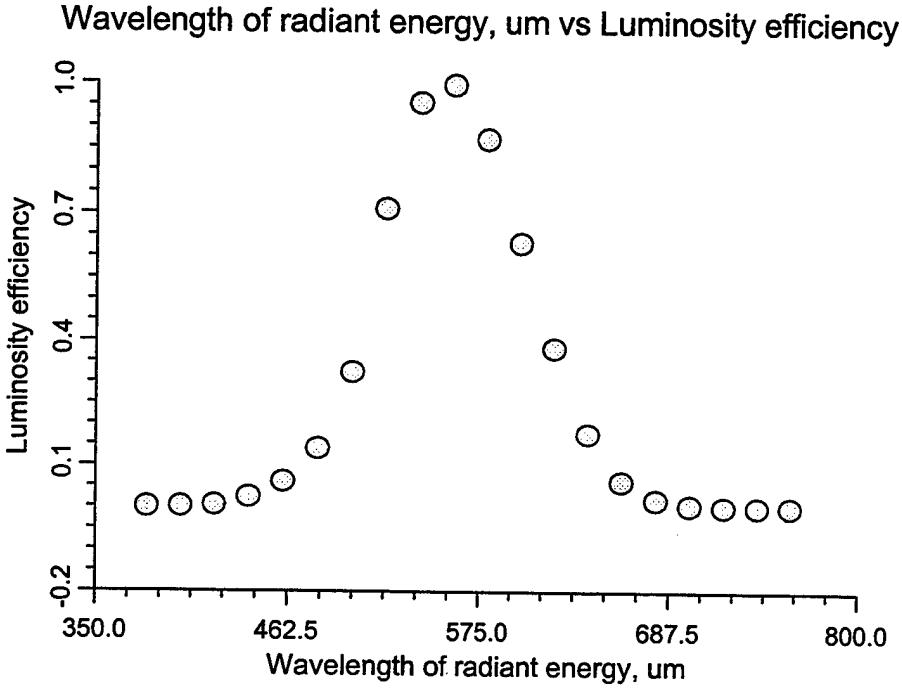

Figure A1: Spectral Response of Eye

1.2 EMISSIVITY, REFLECTANCE, ABSORPTANCE, AND TRANSMITTANCE

Emission, reflection, absorption, and transmission of radiant (solar-spectral) are often treated as surface phenomena. In reality, all of these phenomena must take place within matter. A true black body, by definition, absorbs all incident radiant energy. However, a gray body would depict a ratio of the absorbed to incident energy, which is defined as absorptance '$\alpha(\lambda)$', to be considerably less than unity. This means that the balance of the energy is reflected and transmitted. Diffuse reflectors would have relatively higher absorptance values with less of the incidence energy transmitted and reflected.

Let us assume that a gray body reflecting object(non-blackbody) having an absorptance '$\alpha(\lambda)$' less than unity, is placed within an ideal blackbody cavity. According to the principles of

* Erickson, Ronald, China Lake Report: "Visual Detection of Targets", China Lake, 1965

thermodynamics, the object will reach the temperature 'T' of the cavity and remain at this temperature. At this equilibrium condition, the spectral irradiance at the object surface is equal to the spectral emitted radiance '$M_\lambda(T)$', derived from Planck's Radiation Law as the energy flow rate per wavelength per unit area of a blackbody surface. Yet the power absorbed by the object will equal '$\alpha(\lambda)M_\lambda(T)$'. The remaining power must be apportioned to transmission and reflection. If the object is assumed opaque, the amount reflected can be quantified using the expression [1 - $\alpha(\lambda)]M_\lambda(T)$. Because an object is generally in equilibrium with its surroundings, it must emit as much energy as it absorbs, '$\alpha(\lambda)M_\lambda(T)$' to satisfy Kirchhoff's law. Emissivity '$\varepsilon(\lambda)$' is defined as the ratio of the energy emitted by the surface compared to the energy emitted by an equal area of a blackbody surface at the same temperature.

At the surface of an object where radiant energy at wavelength 'λ' is incident upon the surface, a fraction '$\alpha(\lambda)$' is absorbed, a fraction '$\rho(\lambda)$' is reflected, and a fraction '$\tau(\lambda)$' is transmitted. For most materials, the radiant absorbing value '$\alpha(\lambda)$' is almost constant with change in incidence angle. But the wavelength dependent reflecting and transmitting radiant energy rates per unit area will change with incidence angle, based on the nature of the optical characteristics of the materials. Because energy must be conserved we have;

$$\alpha(\lambda) + \rho(\lambda) + \tau(\lambda) = 1 \qquad \text{(A-3)}$$

The reflection may occur at the surface by either specular (glint) or diffuse reflection, or it may return from within the material by scattering if the material is a translucent, non-homogeneous medium.

In summary, the incident, reflected, and emitted energy must be considered external to the object surface. Internal to the object surface, there is absorbed, transmitted, and scattered energy.

1.3 ATMOSPHERIC EXTINCTION EFFECTS

There are three atmospheric processes responsible for the attenuation of transmitted optical images and electro-optical energy such as solar glint. They are 1) aerosol extinction, 2) molecular absorption, and 3) turbulent distortion (scintillation and beam wander). Light propagating through the atmosphere is not only scattered and absorbed by aerosols and molecules, but the wave fronts are deflected and distorted by turbulence.

1.3.1 OPTICAL PARAMETERS

The two atmospheric optical properties of primary interest are total extinction and the refractive index structure function parameter, 'C^2_N'. The extinction has several components: molecular scattering and absorption ($\beta = \beta_s + \beta_a$), and aerosol scattering and absorption ($\alpha = \alpha_s + \alpha_a$). The extinction parameter values correlate to the loss of light energy as it is scattered out of the beam or absorbed by the molecule and particulate constituents of the atmosphere during transmission. A combination of Bouguer's and Beer's laws can theoretically quantify the level of absorption of transmitted radiant energy '$\Phi(\lambda)$' over a distance 'R', based on the nature of the absorption medium 'α_m' and wavelength of the original transmitted energy '$\Phi_0(\lambda)$' using the following expression,

$$\Phi(\lambda) = \Phi_0(\lambda) \exp [-\alpha_m(\lambda)R] \qquad \text{(A-4)}$$

The distortion and tilt of image wave fronts by atmospheric turbulence is represented by 'C^2_N'. We can write 'C^2_N' as a function of temperature 'C^2_T' and water vapor '(C^2_Q)' turbulence parameters as follows:

$$C^2_N = (79x10^{-6}P/T^2)^2(C^2_T + 0.113\ C_{TQ} + 3.2x10^{-3}\ C^2_Q) \qquad \text{(A-5)}$$

where 'P' is the pressure in milli-bars, 'T' the absolute temperature, and 'C_{TQ}' the temperature humidity co-spectral structure function parameter. The refractive index parameter 'C^2_N' can be derived in three ways: 1) optical measurement, 2) measurement of 'C^2_T, 'C_{TQ}' and 'C^2_Q', and 3) calculation of 'C^2_T', 'C_{TQ}' and 'C^2_Q' from bulk meteorological data made up of water temperature, air temperature, humidity and wind speed.

The total extinction ($\alpha + \beta$) can be measured optically by determining the reduction in beam intensity over some suitable optical path. The separate components can be calculated from meteorological data. The molecular extinction values can be extracted from a LOWTRAN model and database developed by the Air Force Geophysics Laboratory (Selby et. al, 1978). The aerosol extinction can be calculated from the aerosol spectral density 'N(r)', as follows;

$$\alpha = \int_0^\infty 2\pi r^2\, E(n,\lambda)\, N(r)\, dr \qquad \text{(A-6)}$$

where r is the particle radius, $E(n,\lambda)$, the total scattering efficiency at wavelength 'λ' and refractive index 'n'.

It was hoped that glint readings taken over distances from the spherical and cylindrical reflecting sources would include the respective total extinction effects. Thus the extinction parameter values could be derived using explicit filtering expressions and compared to an existing U.S. Air Force LOWTRAN database.

The spectral frequency and level of amplitude of the scintillation and shape of the spectral transmission signature could not be quantified.

1.4 CONTRAST RATIOS

A highly developed sensitivity of the eye is its ability to detect a small difference in luminance. This difference is called contrast sensitivity or liminal contrast. Contrast 'C' for a given set of conditions is defined as,

$$C = (L_B - L_0)/L_A \qquad \text{(A-7)}$$

where 'L_0' and 'L_B' are the object's or reflecting surface's and background luminances respectively. The luminance to which the eye is adapted is 'L_A'. When the reflecting object and background fill the field of view of the eye, 'L_A' is determined by 'L_0' and 'L_B'. When the reflecting object and background illuminated areas are approximately equal in size, then,

$$L_A \cong 1/2(L_B + L_0) \qquad \text{(A-8)}$$

If the size of the reflecting or luminous object is small compared to that of the background, which is true regarding the eye armor reflecting surface to background size ratios, then the eye adaptation response approximates the background illumination

$$L_A \cong L_B. \qquad \text{(A-9)}$$

1.4.1 GLINT CONTRAST RATIO MODEL

The application of the imaging detector for taking glint and background reflection measurements will help verify a U.K. contrast ratio model* that considers spectrally resolved and spectrally integrated applications. This model has some basic limitations in realistically calculating glint attenuation over distance. It excludes the effects of atmospheric extinction on transmitted glint energy. Furthermore, it excludes the effects of the optical surface's reflection coefficients on the level of solar spectral energy reflecting from a surface as a function of incidence/reflection angle and wavelength. It does include the effects of the radius of curvature of a reflecting source.

The model assumes the glint reflection viewed by an observer is a point source and the background an extended object. The point source application assumes that the spectral intensity decreases as an inverse square of distance. Glint to background spectrally resolved contrast ratios are independent of changes in solar brightness since the glint and background components change simultaneously.

The U.K. model has the potential for being used as a glint threshold distance model if the surface properties of a reflecting surface and atmospheric extinction are taken into account.

1.4.1.1 SPECTRALLY RESOLVED RELATIVE INTENSITY

To derive the representative expression for spectrally resolved relative intensity we need to examine the relationships of the perceived intensity of glint from a reflecting surface(goggles) and solar intensity from a background.

Let the goggles curved surface have radius 'r' such that its focal length is 'r/2'. The goggles will reflect sunlight into a diverging cone of half angle (D/2)/(r/2) = (D/r), where 'D' equals cone diameter at reflecting surface. This means that the reflected cone at range 'R' has a radius of (R)(D/r).

Let glint reflection intensity from goggle surface = $I_0(\lambda,\alpha)\rho(\lambda,\alpha)=I_{gog}(\lambda)$
where, solar intensity function = $I_0(\lambda,\alpha)$, incident to goggle surface at angle (α) at visual wavelength (λ). Also, goggle reflectivity coefficient function = $\rho_g(\lambda,\alpha)$ at visual wavelength (λ) and incident angle (α).
Then, the reflected power/unit area at range R is defined as follows.

$$\text{power/unit area} = [I_0(\lambda,\alpha)\rho_g(\lambda,\alpha)\pi(D^2)/4\ ]/\ [\pi(R^2D^2/r^2] = I_{gog}(\lambda)r^2 / 4R^2 \qquad \text{(A-10)}$$

* RI Young, RC Hollins, T Holloway "Simple Model for Predicting Glint to Background Contrast Ratios, Optical Glint Studies US and U.K. Joint Venture", DERA, U.K., July 1997

Now the sensor receives power over detector area 'A_d' but lacks the angular resolution to form a proper image of glint. Thus glint appears as a feature of the detector angular width 'θ_d' resolution. Since the perceived glint intensity as seen by the detector is equivalent to (received power/angular width squared), then the perceived glint intensity at detector can be defined as 'I_{gd}'. The detector glint intensity level can now be expressed as:

$$I_{gd}(\lambda) = I_{gog}(\lambda) r^2 A_d / 4\theta_d^2 R^2 \qquad \text{(A-11)}$$

which depends on angular resolution 'θ_d' of sensor. Since point source theory is applied, the intensity relates inversely to the square of the range or distance 'R' from reflecting source to detector.

The background intensity $I_b(\lambda)$ reflects with diffuse reflectance $\rho_b(\lambda)$ times incident solar intensity $I_0(\lambda)$ into a solid angle '2π'. From a background of area 'A_b', the reflected intensity at range R_0 is

$$I_b(\lambda) = A_b I_0(\lambda) \rho_b(\lambda) / 2\pi R_0^2 = A_b I_b(\lambda) / 2\pi R_0^2 \qquad \text{(A-12)}$$

The power received by the sensor is $(A_d)(I_b)$ where perceived detector area is defined by A_d. Since the background area 'A_b' is sufficiently large for a detector sensor to form a properly resolved image of angular size $(A^{0.5})/ R_0$, then the detector perceived background intensity 'I_{bd}' can be expressed as perceived power/angular width squared.

$$I_{bd}(\lambda) = [R_0^2/A_b] A_d A_b I_b(\lambda) / 2\pi R_0^2 = I_b(\lambda) A_d / 2\pi \qquad \text{(A-13)}$$

Thus the perceived intensity of background by a detector is independent of its angular resolution and the range between background and reflecting source, given the assumption that the diffusion reflection has a '2π' angular domain due to a flat background.

We can now define the intensity of glint relative to the background as perceived by the detector, in terms of spectrally resolved relative intensity, by solving for the contrast ratio '$C_R(\lambda)$' of the previously derived expressions of glint and background reflections 'I_{gd}, I_{bd}'.

$$C_R(\lambda) = [I_{gd}(\lambda)/I_{bd}(\lambda)] = [I_{gog}(\lambda)/I_b(\lambda)](\pi r^2) / [2\theta_d^2 R_0^2] \qquad \text{(A-14)}$$

This spectrally resolved contrast ratio expression is independent of solar intensity but depends on angular resolution of detector source, distance from reflecting source, and optical reflection characteristics of background and reflecting surface. The contrast ratio calculated over distance is based on the inverse square law.

1.4.1.2 SPECTRALLY INTEGRATED RELATIVE INTENSITY

Let us consider a spectrally integrated relative intensity as perceived by a detector with a spectral response function '$f(\lambda)$'. The spectrally integrated contrast ratio 'C_I' can be expressed by

combining the spectrally resolved expression '$C_R(\lambda)$' from the previous section with the integral expressions of ; a) solar energy '$I_0(\lambda,)$' attenuated by the solar zenith angle coefficient function '$Z_c(\lambda,\beta)$' and incident to the goggle and background surfaces, b) background and surface reflectivity coefficient functions '$\rho_b(\lambda)$ and $R_c(\lambda,\alpha)$' and b) spectral response function of detector '$f(\lambda)$'.

Thus the resulting expression is

$$C_I = \left[\frac{\int I_0(\lambda,)Z_c(\lambda,\beta)R_c(\lambda,\alpha)f(\lambda)d\lambda}{\int I_0(\lambda)\rho_b(\lambda)\, f(\lambda)d\lambda} \right](\pi r^2) / [2\theta_d{}^2 R_0{}^2] \qquad \text{(A-15)}$$

This is a useful model for ocular (eye) detection. However, the model is sensitive to solar spectral shifts caused by changes in the optical path of sunlight due to the solar elevation angle coupled with the atmospheric extinction effects.

1.4.1.3 IMPROVED MATHEMATICAL MODEL

The use of a mathematical model for accurately calculating a glint visual domain is significant for designing low reflectivity optical surfaces. This is possible by mathematically describing the attenuation of solar glint energy over the sun to reflecting surface to observer optical path. The attenuation begins with the effects of atmospheric extinction, defined as solar zenith angle coefficients, on the passage of solar energy through the atmosphere at various elevation angles, as depicted by the solar relative intensity versus zenith angle graph* in Figure A2.

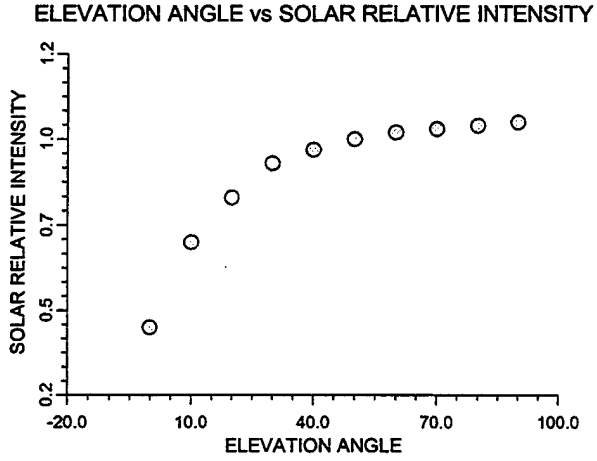

Figure A2: Atmospheric Extinction Effects on Solar Energy

Another attenuation effect along the optical path results from the optical characteristics of the reflecting surface, which depict a relationship between solar incidence/reflection angle and reflection coefficients as shown in the surface reflectivity coefficient graph in Figure A3.

* Kreith, Frank, Principles of Solar Engineering. Washington, DC, McGraw

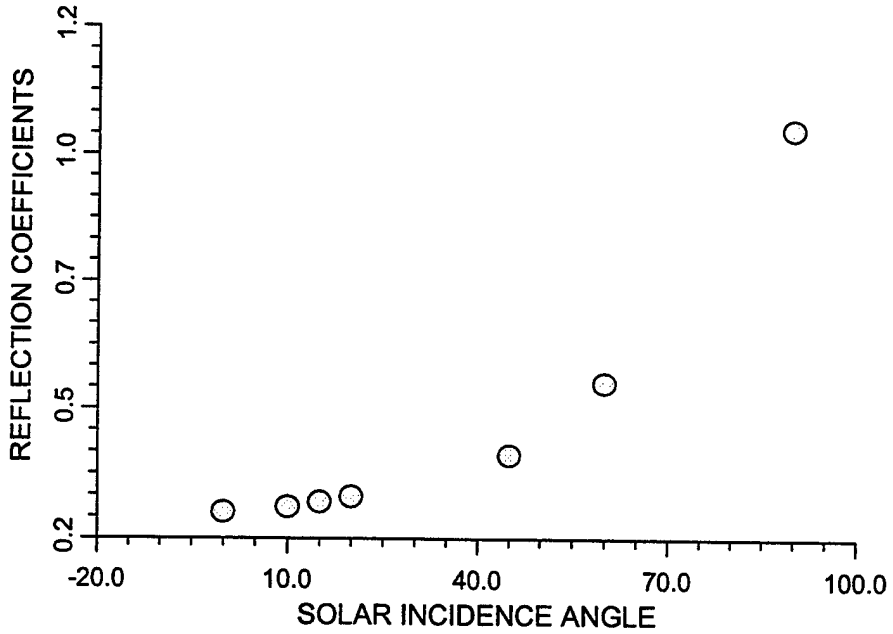

Figure A3: Reflectivity Characteristics of Eye Armor Surface

The whole idea using this model as an iterative design tool lies with the fact that changes in the reflectivity coefficients associated with optical surface properties changes of a reflecting surface will affect glint threshold distance calculations.

The final segment of the optical path is the atmospheric absorption and scattering extinction effects on reflected solar spectral energy transmitted to an observer detecting source, based on humidity and particulate levels. Atmospheric turbulence effects on transmitted solar energy are not considered. Refer to previous section 1.3.1: 'Optical Parameters' for details. A combination of Bouguer's, Lambert's and Beer's laws can theoretically quantify the level of absorption of transmitted radiant energy '$\Phi(\lambda)$' over a distance 'R', based on the nature of the absorption medium 'α_m' and wavelength of the original transmitted energy '$\Phi_0(\lambda)$' using the following expression.

$$\Phi(\lambda) = \Phi_0(\lambda) \exp [-\alpha_m(\lambda)R] \qquad \text{(A-16)}$$

1.4.1.3.1 DETECTOR POWER PER ANGULAR RESOLUTION

The observer will view the level of solar brightness contrast of a reflecting source relative to background in terms of (power)/(angular detection width squared). Also, the contrast ratio spectrally resolved and integrated expressions developed in the previous sections 1.4.1.1 and 1.4.1.2. will be modified to include the optical characteristics of the reflecting surface and the effects of atmospheric extinction. The glint reflection intensity from goggle surface '$I_{gog}(\lambda)$' will be modified as the product of the zenith solar intensity '$I_0(\lambda)$', the solar zenith angle coefficient function '$Z_c(\lambda,\beta)$', and the surface reflectivity coefficient function $R_c(\lambda,\alpha)$.

1.4.1.3.1.1 SPECTRALLY RESOLVED APPROACH

The spectrally resolved contrast ratio expression can now be expressed as follows:

$$C_R(\lambda) = [I_{gd}(\lambda)/I_{bd}(\lambda)] = [I_0(\lambda)Z_c(\lambda,\beta)R_c(\lambda,\alpha)/I_b(\lambda)]\{\exp[-\alpha_m(\lambda)R_0]\}(\pi r^2) / [2\theta_d^2 R_0^2] \quad \text{(A-17)}$$

where; $C_R(\lambda)$ = contrast ratio (wavelength dependent)

$I_{gd}(\lambda)$ = goggles reflected solar intensity incident to detector

$I_{bd}(\lambda)$ = background reflected solar intensity incident to detector

$I_0(\lambda)$ = zenith solar intensity (wavelength dependent)

$Z_c(\lambda,\beta)$ = solar zenith angle coefficient function (wavelength and zenith angle(β) dependent)

$R_c(\lambda,\alpha)$ = normalized surface reflectivity coefficient function (wavelength and incident angle(α) dependent)

$I_b(\lambda)$ = reflected background solar intensity

$\alpha_m(\lambda)$ = atmosphere total extinction coefficient

R_0 = distance or range observer from glint reflecting source

r = radius of curvature of goggles (gently sloping)

θ_d = angular resolution or spread of detecting source

If we mathematically solve the previous expression for range 'R' we get

$$R_0 = (r/\theta_d)\{[I_0(\lambda)Z_c(\lambda,\alpha)R_c(\lambda,\alpha)/I_b(\lambda)]\{\exp[-\alpha_m(\lambda)R_0]\}\pi /2C(\lambda)\}^{0.5} \quad \text{(A-18)}$$

By arbitrarily setting a) the threshold contrast ratio $C(\lambda)$ to a value i.e., '10', b) the extinction coefficient '$\alpha_m(\lambda)$' to a corresponding level of humidity, c) a solar elevation angle coefficient '$Z_c(\lambda,\alpha)$' to the solar elevation angle, and d) a normalized reflectivity function '$R_c(\lambda,\alpha)$' to represent the specific reflecting surface, assuming a detector angular resolution, a visual domain bounded by a locus of visual threshold points across a range of incidence angle values can be generated by solving for the range R_0. Changing the reflecting surface's optical characteristics, would result with changes in the size and shape of the generated visual threshold domain.

On perfectly clear days the extinction coefficient 'α_m' approaches zero in value such that the exponential expression has a value of one. If there are varying levels of humidity, then the range R_0 would have to be solved iteratively.

The advantages of using this approach is that the contrast ratio is independent of solar intensity but depends on detector source's angular resolution. The intensity decreases as the inverse square of range. Regarding the reflecting surface geometry, the reflecting surface effective radius of curvature is the square root of the product of the radii components

1.4.1.3.1.2 SPECTRALLY INTEGRATIVE APPROACH

We can use the spectrally integrative approach even though the contrast ratio is sensitive to spectral changes such as diurnal spectral shifts. The expression would be an integral over the 0.4

- 0.7μm eye photo visual region of the solar spectrum of the previous spectrally resolved expression.

It is expressed as

$$C_I = \left[\frac{\int I_0(\lambda)Z_c(\lambda,\beta)R_c(\lambda,\alpha)f(\lambda)d(\lambda)}{\int I_0(\lambda)\rho_b(\lambda)f(\lambda)d(\lambda)}\right]\{\exp[-\alpha_m(\lambda)R_0]\}(\pi r^2) / [2\theta_d^2 R_0^2] \quad \text{(A-19)}$$

where; $I_0(\lambda)$ = zenith solar intensity (wavelength dependent)
$Z_c(\lambda,\beta)$ = solar elevation angle coefficient(wavelength and zenith angle dependent)
$R_c(\lambda,\alpha)$ = normalized surface reflectivity function (wavelength and incident angle dependent)
$\rho_b(\lambda)$ = background reflectivity coefficients
$\alpha_m(\lambda)$ = atmosphere total extinction coefficient
R_0 = distance or range observer from glint reflecting source
r = radius of curvature of goggles (gently sloping)
θ_d = angular resolution or spread of detecting source
$f(\lambda)$ = detector spectral response function

1.4.1.3.1.3 IMPROVED MODEL SOFTWARE

By writing an algorithm to quantify and pictorially show these results in a software hardware configuration, we have an accurate reflecting surface design tool to aid in the design and applications of existing and leading edge reflection technologies.

A more accurate interpretation of the attenuation of transmitted solar energy along its optical path enhances realism to the model design applications.

1.4.1.4 CONTRACTOR MODEL

The contractor developed glint threshold domain algorithm that the field trial results were to validate and modify is based on a sea navigation equation* that relates threshold intensity of light to range. The candlepower 'C' in candles at the visual threshold of a steady point source seen against a background brightness level 'b' milli-micro-lamberts (mμL) at range 'r'(sea miles) through an atmosphere of attenuation 'a' per sea mile is expressed as

$$C = .0037(1 + b)^{1/2} r^2 a^{-r} \quad \text{(A-20)}$$

which is valid within a factor of 3 for 'b' values that range from total darkness to full daylight.

*Forsythe, William Elmer, Smithsonian Physical Tables, 9th Revised Edition, Washington, D.C., Smithsonian Institution Press, 1956

The model calculates the value of 'C' by multiplying the integrally averaged results of the solar zenith spectral function, the solar zenith angle coefficient, and a range of surface reflection coefficients. It assumes a perfectly clear day so that the atmospheric extinction expression 'a^{-T}' is equal to 1. Thus no iterations are necessary during the solution process.

The visual threshold locus of points are calculated by solving for the corresponding threshold range 'R' values to establish the visual threshold domain, based on a range of optical surface reflectivity coefficients which correspond to a range of glint incidence/reflection angles. Only two background brightness factors representing typical daytime and nighttime reflections are used.

Because distance between reflecting source and observer is substantial, glint reflection is considered a point source. Thus the inverse square law ($1/R^2$) is used to calculate the glint threshold locus of points. The model uses a signaling factor of 100 and a 2π r(0.56/360)h reflecting increment of the reflecting surface. The radius of curvature is 'r', the height of the goggles is 'h' and the 0.56 is the angular width of the sun.

Although field trial validation and verification is necessary to add breadth to the model by considering the effects of different geometric surfaces, atmospheric extinction effects on glint signature and angular discernment of the detector source, the model still can be used as a rough cut 'relative measures' design tool when applying reflection technologies to optical surfaces.

APPENDIX B.

DATA SPREADSHEETS

GLINT FIELD TRIALS, MALVERN, U.K.

Table B.1 Dielectric Stack Cylindrical Lens Data Using 670 nm Filter

DIELECTRIC STACK CYLINDRICAL LENS EYE ARMOR DATA
(Narrow Band Pass 670 nm Filter)

Trial No.	Range (meters)	Neutral Density	LUX (reflected)	Contrast Ratio	Peak Signal	Air Temp. Degr (C)	Relative Humid(%)	Dew Point Temp(C)	Air Press. (mb)	Wind Vel. (m/s)
1	1100	1	1119	9.5	163	24	45	11.3	966	1.65
2	1100	1.3	900	4.6	35	24	45	11.3	966	1.65
3	1100	1	660	2.9	35	24	45	11.3	966	1.65
4	1100	1.3	1100	8.9	89	24	45	11.3	966	1.65
5	1100	1.3	1199	10.7	73	24	45	11.3	966	1.65
6	1100	1.3	1195	15	126	24	45	11.3	966	1.65
7	1000	0	1000	off scale	255	24	45	11.3	966	1.65
8	1000	1	1300	11.5	143	24	45	11.3	966	1.65
9	1000	1	1289	3.82	62	24	45	11.3	966	1.65
10	900	0	1060	off scale	offscale	24	45	11.3	966	1.65
11	900	1.3	900	25.7	113	24	45	11.3	966	1.65
12	900	1.3	1082	11.5	85	24	45	11.3	966	1.65
13	900	1	1150	3.82	71	24	45	11.3	966	1.65
14	800	1	800	22	255	24	45	11.3	966	1.65
15	800	1.5	850	34.2	178	24	45	11.3	966	1.65
16	800	1.5	1050	32	152	24	45	11.3	966	1.65
17	800	1.5	1023	22.8	91	24	45	11.3	966	1.65
18	800	1.5	1057	25.3	101	24	45	11.3	966	1.65
19	800	1.5	1047	off scale	offscale	24	45	11.3	966	1.65
20	800	1.5	950	21	1	24	45	11.3	966	1.65
21	800	1	500	13	13	24	45	11.3	966	1.65
22	700	1.5	1030	30	156	24	45	11.3	966	1.65
23	700	1.5	1090	off scale	offscale	24	45	11.3	966	1.65
24	700	1.5	1025	34	186	24	45	11.3	966	1.65
25	700	1.5	1030	32	82	24	45	11.3	966	1.65
26	700	1.5	1015	66	239	24	45	11.3	966	1.65
27	650	1.5	984	15.7	85	24	45	11.3	966	1.65
28	650	1.5	975	saturated	255	24	45	11.3	966	1.65
29	650	1.5	950	20	117	24	45	11.3	966	1.65
30	650	1.5	1010	17	77	24	45	11.3	966	1.65
31	650	1.5	1005	21	114	24	45	11.3	966	1.65
32	650	1.5	1050	off scale	246	24	45	11.3	966	1.65
33	650	1.5	1057	48	258	24	45	11.3	966	1.65
34	600	1.5	1032	43	255	24	45	11.3	966	1.65
35	600	2	1031	off scale	offscale	24	45	11.3	966	1.65
36	600	1.5	980	39	175	24	45	11.3	966	1.65
37	600	1.5	980	19	75	24	45	11.3	966	1.65
38	600	1.5	950	realign	185	24	45	11.3	966	1.65
39	600	1.5	950	29	86	24	45	11.3	966	1.65

Notes:

1). No correlation between the light meter lux readings and peak signal level. Lux of light meter varied too quickly to be coordinated with CCD readouts.

2). Neutral Density equals optical density across CCD camera.

3). Contrast ratio equates to brightness of reflecting surface to background.

4). Peak Signal equals photoelectric conversion in CCD camera using binary octal bit scale (0 - 255).

5). Large proportion of data variability is unwanted type.

6). Meteorological data located in columns 7 -11represent average values taken within time interval of 11:52 - 15:54 of day 9 during which glint trials were executed.

Table B.2 Spherical Lens (U.K.,ABLES) Eye Armor Data Using Visual Spectrum Filter

SPHERICAL LENS EYE ARMOR DATA
Visual Spectrum Filter

Trial	Range (meters)	Neutral Density	LUX (reflected)	Contrast Ratio	Peak Signal	Air Temp. (C)	Relative Humid(%)	Dew Point Temp(C)	Air Press. (mb)	Wind Vel. (m/s)
1	20	1	880	saturated	256	22.3	57.4	13.4	970	1.65
2	20	2.3	1100	42	109	22.3	57.4	13.4	970	1.65
3	20	2.3	930	45	107	22.3	57.4	13.4	970	1.65
4	20	2.3	840	48	105	22.3	57.4	13.4	970	1.65
5	20	0	n/a	saturated	256	19.6	75.8	16	963	3.5
6	20	1.5	n/a	12	152	19.6	75.8	16	963	3.5
7	30	1	1190	saturated	256	22.3	57.4	13.4	970	1.65
8	30	2	1120	8.3	114	22.3	57.4	13.4	970	1.65
9	30	2	1094	8.4	114	22.3	57.4	13.4	970	1.65
10	30	2	1215	10.4	123	22.3	57.4	13.4	970	1.65
11	30	2	n/a	45	136	19.6	75.8	16	963	3.5
12	30	0	n/a	saturated	256	19.6	75.8	16	963	3.5
13	40	1	840	saturated	256	22.3	57.4	13.4	970	1.65
14	40	2	930	5.2	76	22.3	57.4	13.4	970	1.65
15	40	2	1005	5.4	84	22.3	57.4	13.4	970	1.65
16	40	2	985	5.2	82	22.3	57.4	13.4	970	1.65
17	40	0	n/a	saturated	256	19.6	75.8	16	963	3.5
18	40	1.5	n/a	11	131	19.6	75.8	16	963	3.5
19	50	1	n/a	6	166	19.6	75.8	16	963	3.5
20	50	0	n/a	saturated	256	19.6	75.8	16	963	3.5
21	50	1	1015	saturated	256	22.3	57.4	13.4	970	1.65
22	50	2	790	3.9	44	22.3	57.4	13.4	970	1.65
23	50	2	930	3.9	50	22.3	57.4	13.4	970	1.65
24	50	2	828	4.2	51	22.3	57.4	13.4	970	1.65
25	60	1	1158	saturated	256	22.3	57.4	13.4	970	1.65
26	60	2	1234	3.4	66	22.3	57.4	13.4	970	1.65
27	60	2	1177	3.7	70	22.3	57.4	13.4	970	1.65
28	60	2	1178	3.3	59	22.3	57.4	13.4	970	1.65
29	60	1.5	1045	2.4	153	22.3	57.4	13.4	970	1.65
30	70	1	1070	1.6	229	22.3	57.4	13.4	970	1.65
31	70	1	1125	1.5	229	22.3	57.4	13.4	970	1.65
32	70	1	1136	1.4	221	22.3	57.4	13.4	970	1.65
33	70	1	1089	1.43	214	22.3	57.4	13.4	970	1.65
34	75	1.3	n/a	4	58	19.6	75.8	16	963	3.5
35	75	0	n/a	saturated	256	19.6	75.8	16	963	3.5
36	85	1.3	n/a	4	67	19.6	75.8	16	963	3.5
37	85	0	n/a	saturated	256	19.6	75.8	16	963	3.5
38	95	0	n/a	saturated	256	19.6	75.8	16	963	3.5
39	95	1.2	n/a	5	100	19.6	75.8	16	963	3.5
40	100	0	n/a	saturated	256	19.6	75.8	16	963	3.5
41	100	0.3	n/a	1.2	160	19.6	75.8	16	963	3.5

Notes:

1). No correlation between the light meter lux readings and peak ht meter signal level. Lux of light varied too quickly, coupled with lag time between lux and CCD readouts.

2). Neutral Density equals optical density across CCD camera.

3). Contrast ratio equates to brightness of reflecting surface to background.

4). Used photopic response filter with spherical eye reflector.

APPENDIX C.

PHOTO VISUALS OF GLINT REFLECTION OFF SPHERICAL AND CYLINDRICAL SURFACES AT VARIOUS DEFINED DISTANCES

Figure C1. Distance of 40 Meters from Spherical Reflecting Surface

Figure C2. Distance of 50 Meters from Spherical Reflecting Surface

Figure C3. Distance of 95 Meters from Spherical Reflecting Surface

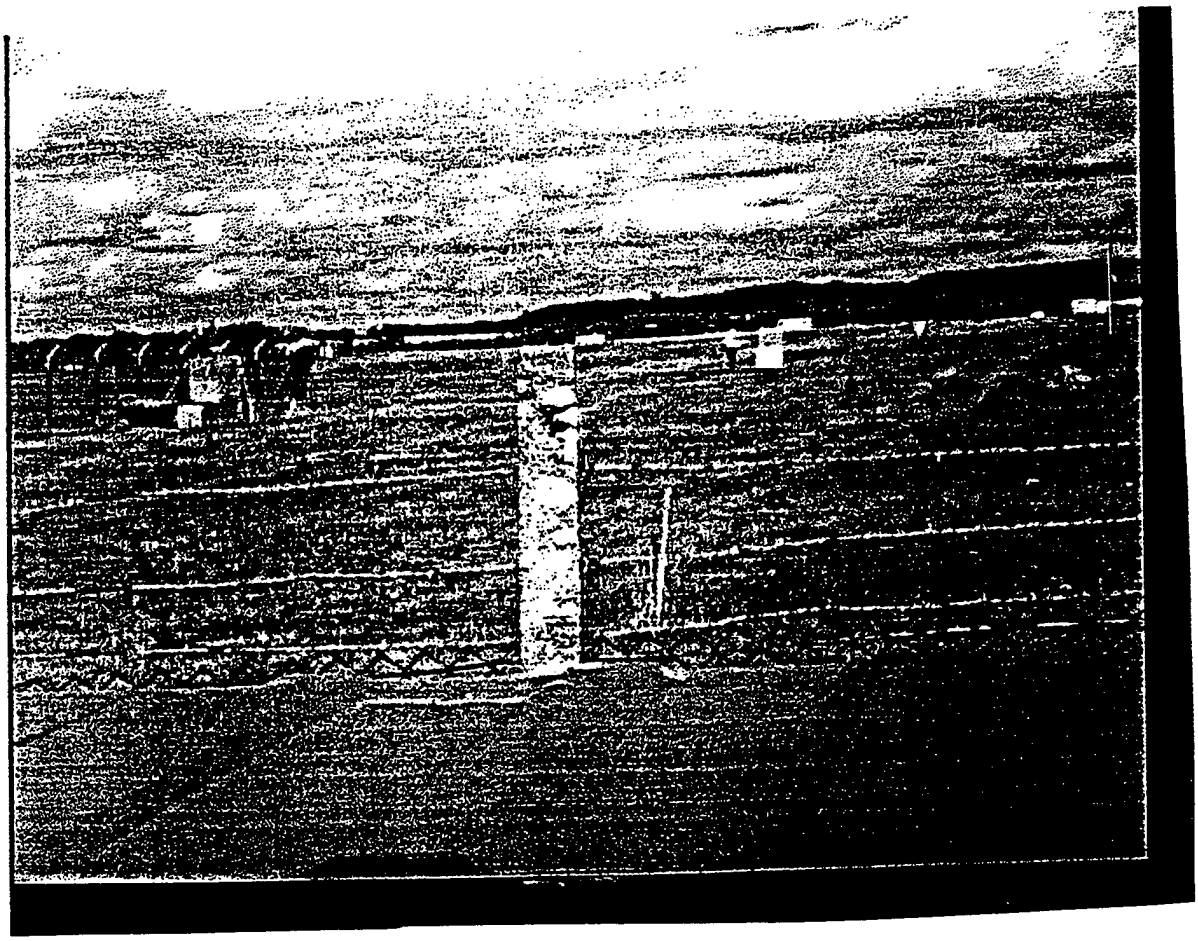

Figure C4. Distance of 150 Meters from Spherical Reflecting Surface

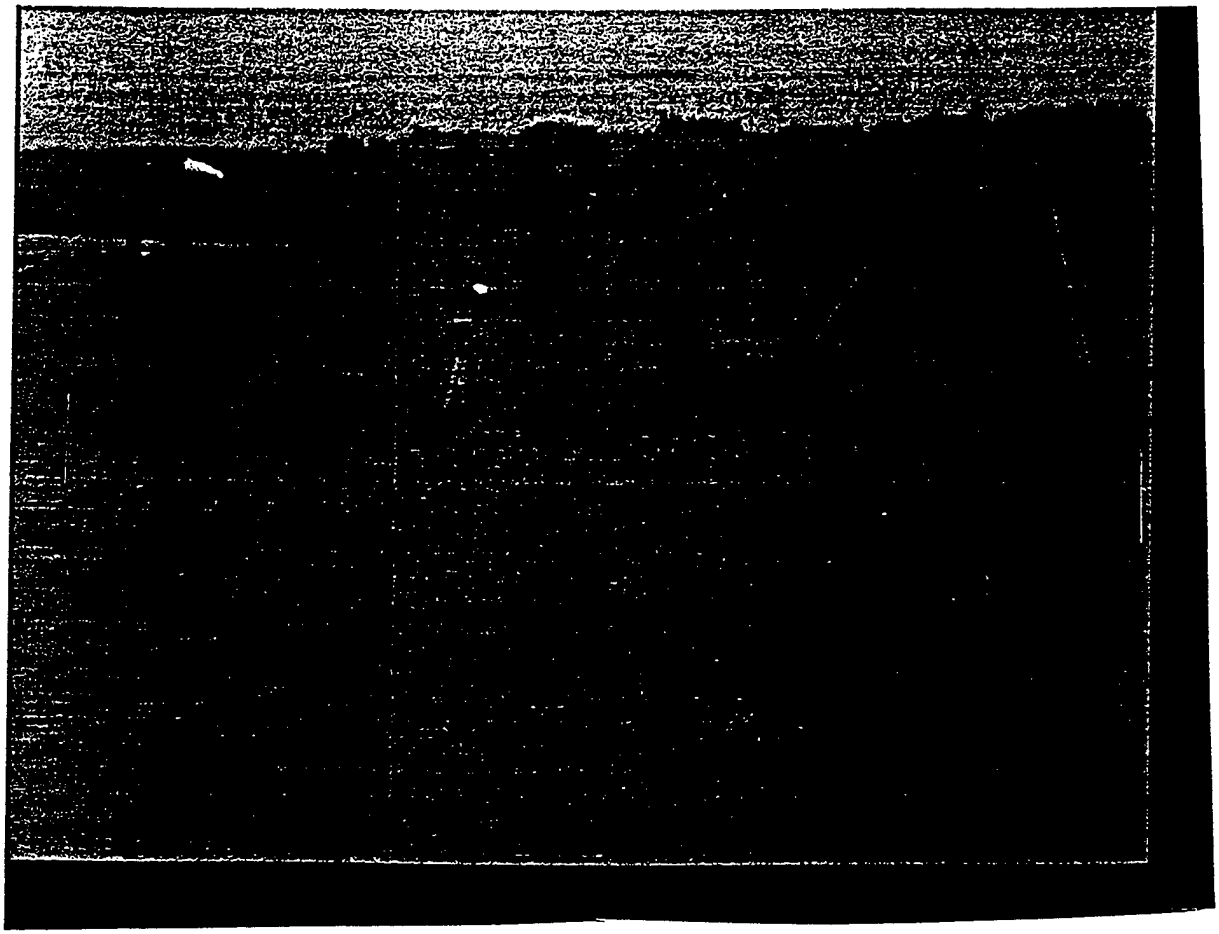

Figure C5. Distance of 100 Meters from Cylindrical Reflecting Surface

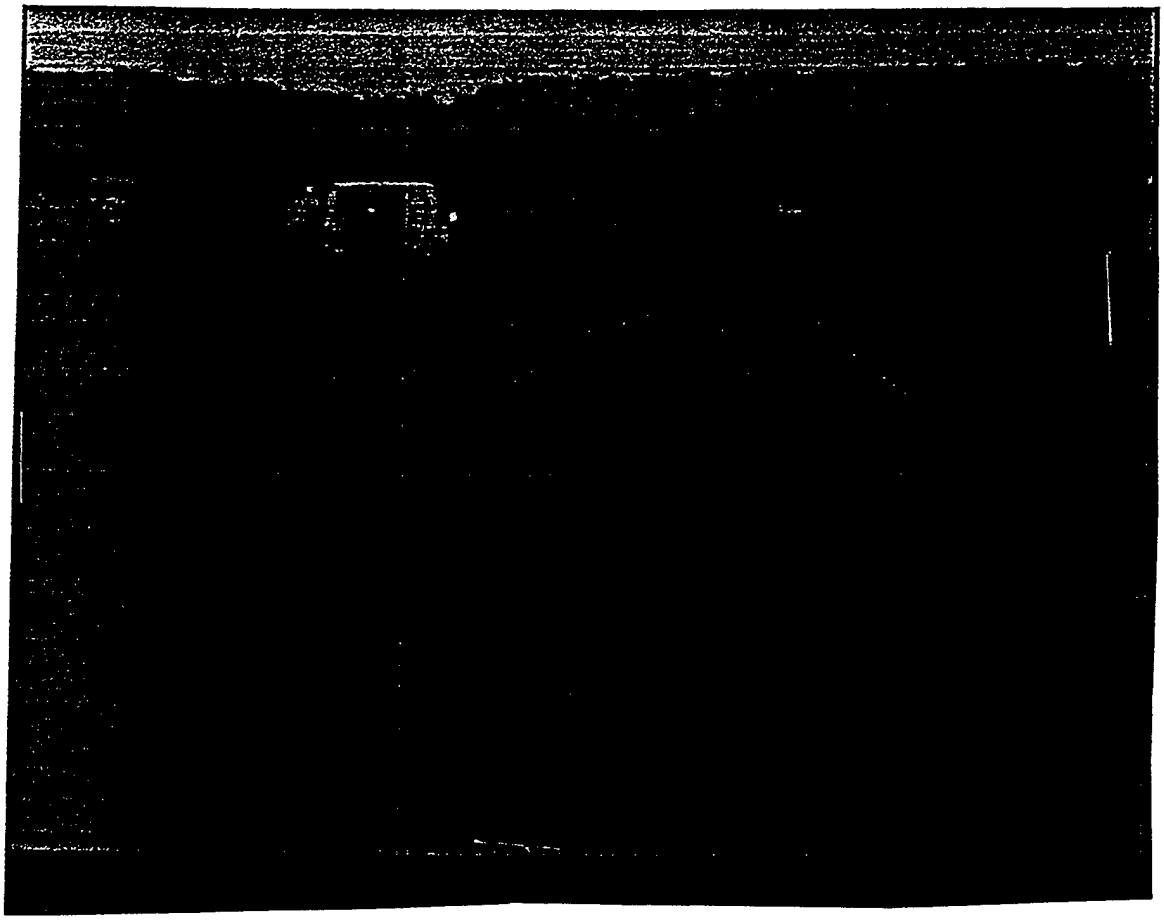

Figure C6. Distance of 190 Meters from Cylindrical Reflecting Surface

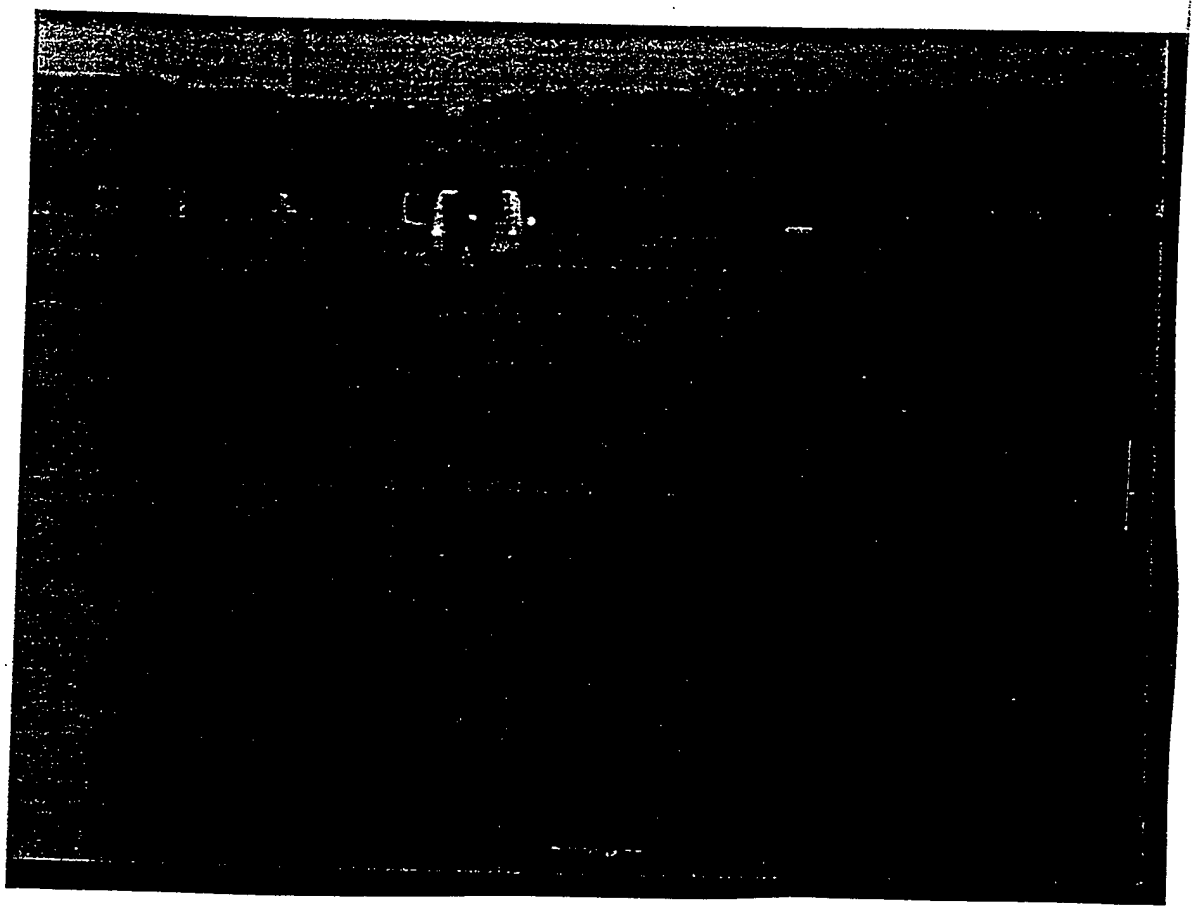

Figure C7. Distance of 250 Meters from Cylindrical Reflecting Surface

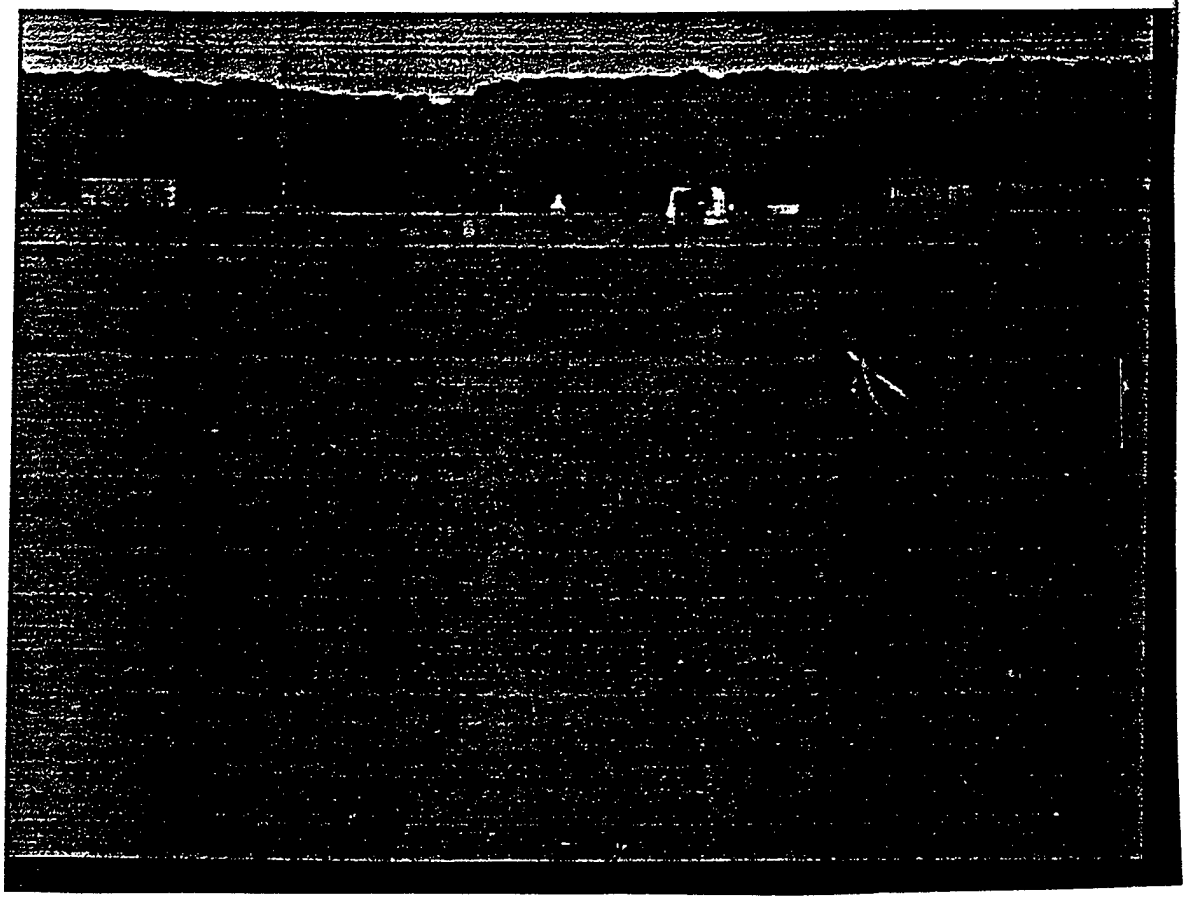

Figure C8. Distance of 400 Meters from Cylindrical Reflecting Surface

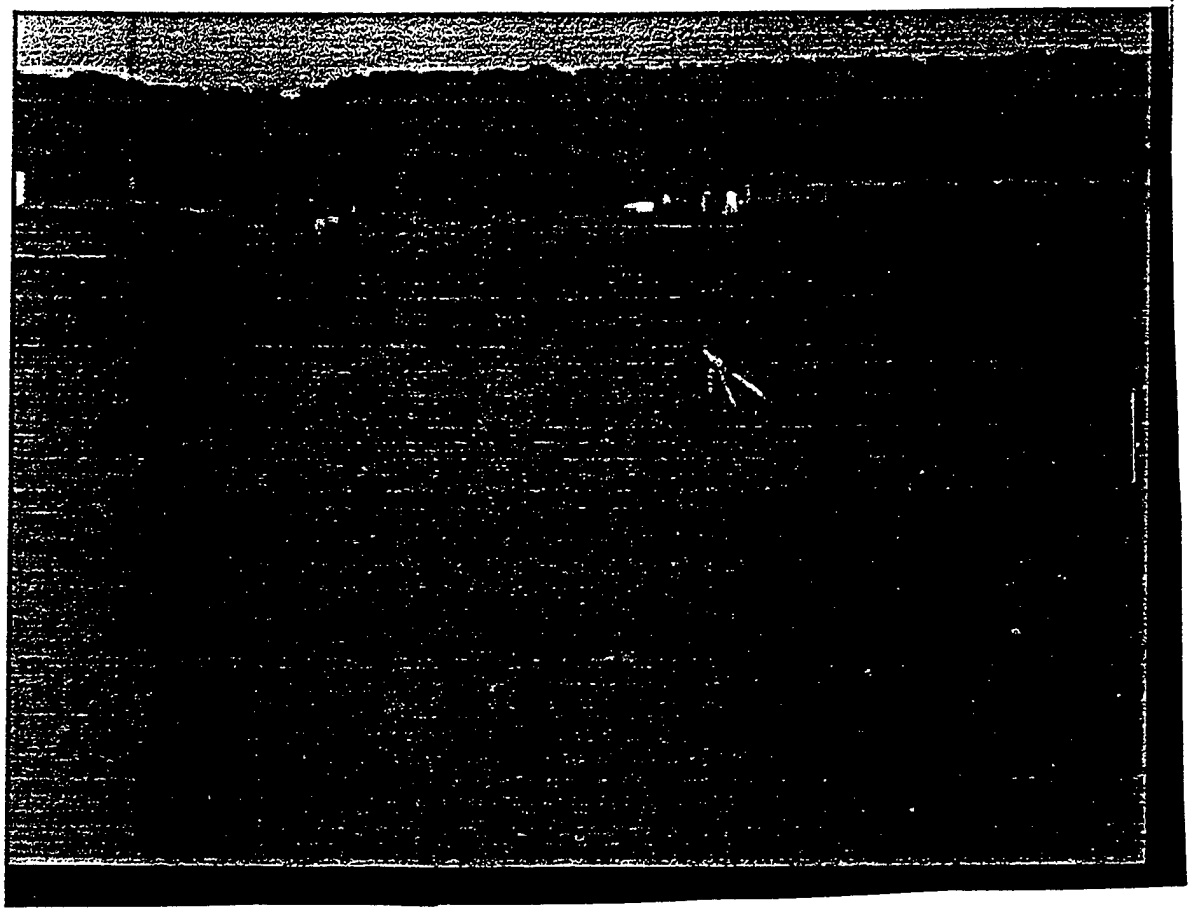

Figure C9. Distance of 600 Meters from Cylindrical Reflecting Surface

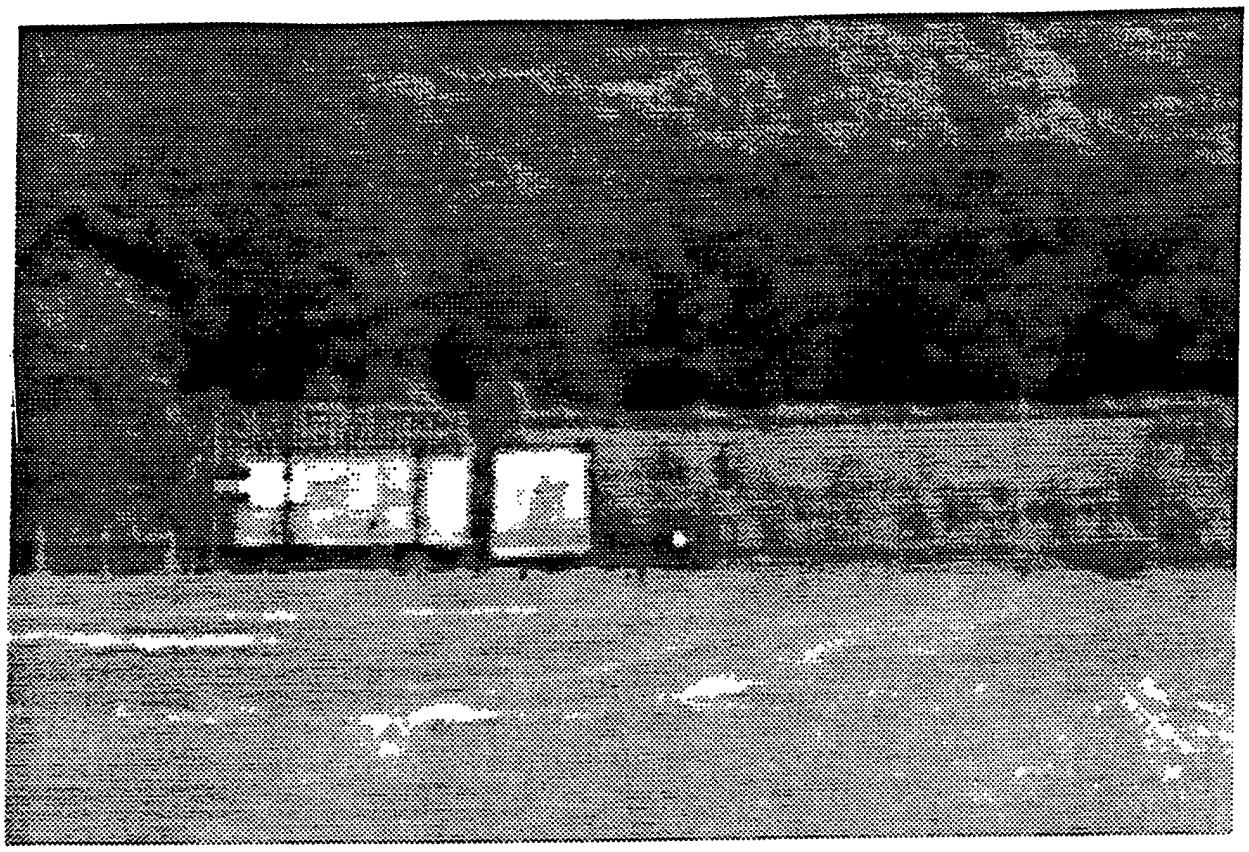

Figure C10. Distance of 1100 Meters from Cylindrical Reflecting Surface